Supplementary Information

Π band dispersion along conjugated organic nanowires synthetized on a metal oxide semiconductor.

Guillaume Vasseur[*,1,2], Mikel Abadia[1], Luis A. Miccio[1,2], Jens Brede[*,1,2], Aran Garcia-Lekue[2,3], Dimas G. de Oteyza[1,2,3], Celia Rogero[1,2], Jorge Lobo-Checa[1,4,5] and J. Enrique Ortega[1,2,6]

[1.] *Centro de Física de Materiales (CSIC/UPV-EHU)-Materials Physics Center (MPC), Paseo Manuel Lardizabal 5, 20018 San Sebastián, Spain.*
[2.] *Donostia International Physics Center, Paseo Manuel Lardizabal 4, 20018 San Sebastián, Spain.*
[3.] *Ikerbasque, Basque Foundation for Science, 48011 Bilbao, Spain.*
[4.] *Instituto de Ciencia de Materiales de Aragón (ICMA), CSIC-Universidad de Zaragoza, 50009 Zaragoza, Spain.*
[5.] *Departamento de Física de la Materia Condensada, Universidad de Zaragoza, 50009 Zaragoza, Spain.*
[6.] *Departamento Física Aplicada I, Universidad del País Vasco, 20018 San Sebastián, Spain*

* Corresponding authors
g.vasseur.univ@gmail.com
dr.jens.brede@gmail.com

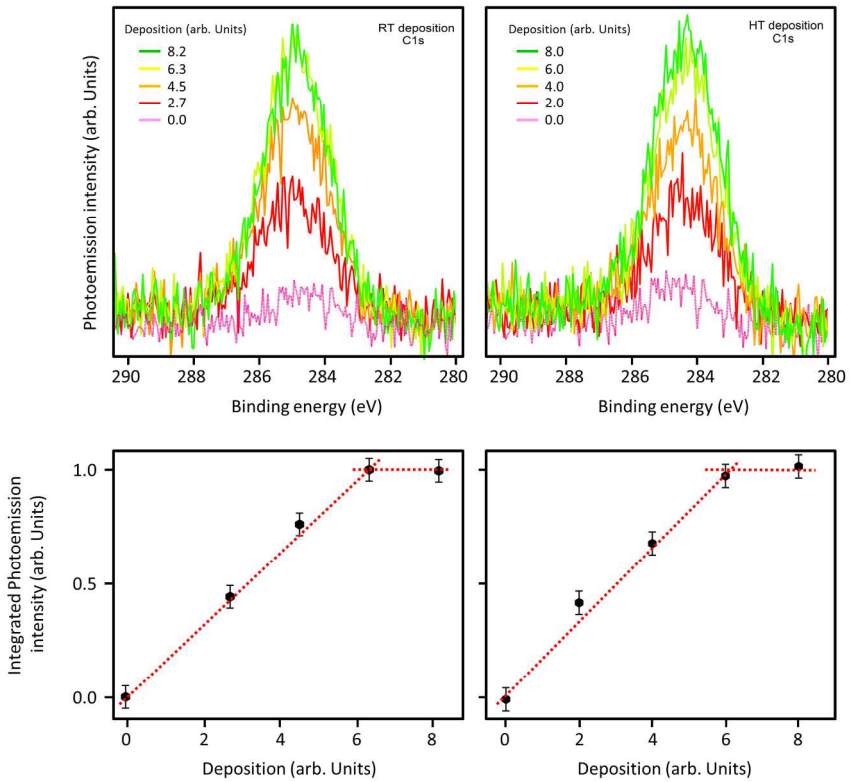

Figure S1: Self-limited growth of supramolecular and polymeric phases. (a,b) Evolution of the XPS spectra of the C1s core level as function of DBTP deposition onto a substrate kept at room temperature (a) and high temperature (b). (c,d) Evolution of the integrated signal as function of deposition, respectively associated to (a,b). The deposition is given by the evaporation time normalized with the molecular rate read on a quartz micro-balance.

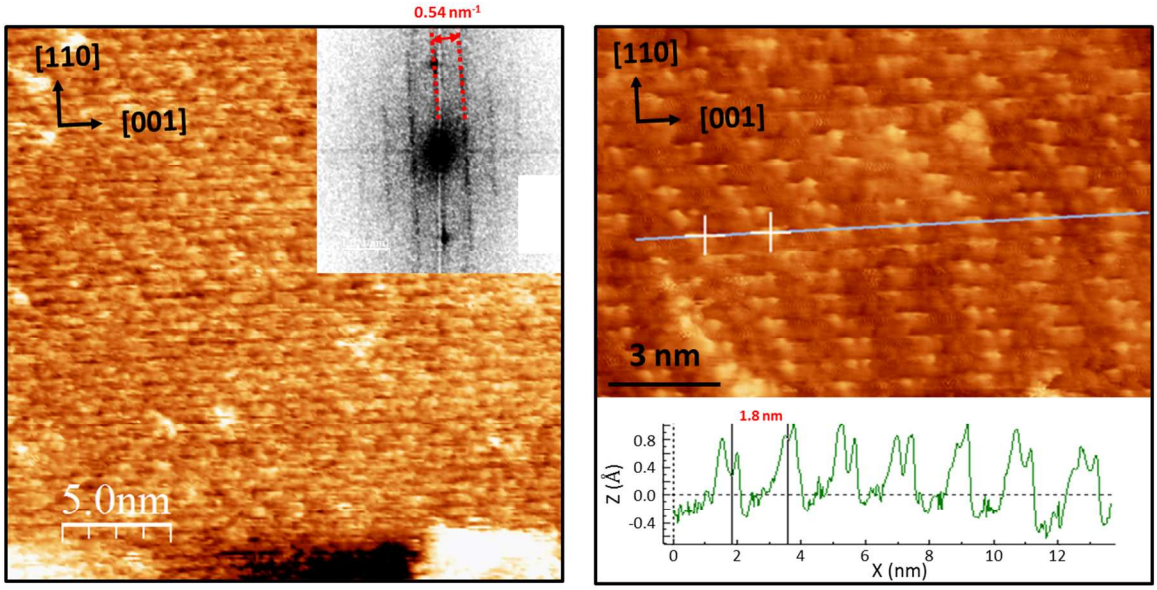

Figure S2: Additional STM images of the supramolecular phase. The inset in the left panel corresponds to the 2D Fourier transform of the image. The one in the right panel display a height profile corresponding to the grey line.

Note 1: Geometry optimization of the DBTP molecule.

The geometry optimization of the different molecular configurations was carried out using density functional theory (DFT), as implemented in the VASP code[1-3]. Inner electrons were described employing the projector augmented wave (PAW) method[4], and valence electrons were expanded in plane waves with an energy cutoff of 400 eV. The optB88-vdW functional[5], which accounts for non-local corrections, was adopted for the exchange and correlation potential. The Gamma point was selected for sampling the three-dimensional Brillouin zone. Isolated molecules as well as molecular dimers were fully relaxed, until residual forces were less than 0.02 eV/Å. According to this method, two energetically equivalent conformations of the free standing DBTP molecules were found, revealing a twisted conformation with C2h and D2 symmetry (Supplementary figure 2). In both cases, the twist angle (θ) is equal to 37.5° and the length (L) of the molecule, i.e. Br-Br distance, equal to 15.21 Å. The interaction between two molecules facing each other along the same axis was investigated for both conformations (Supplementary figure 3), revealing that supramolecular interactions stabilize the inter-molecular distance with a Br-Br distance of 3.8 Å.

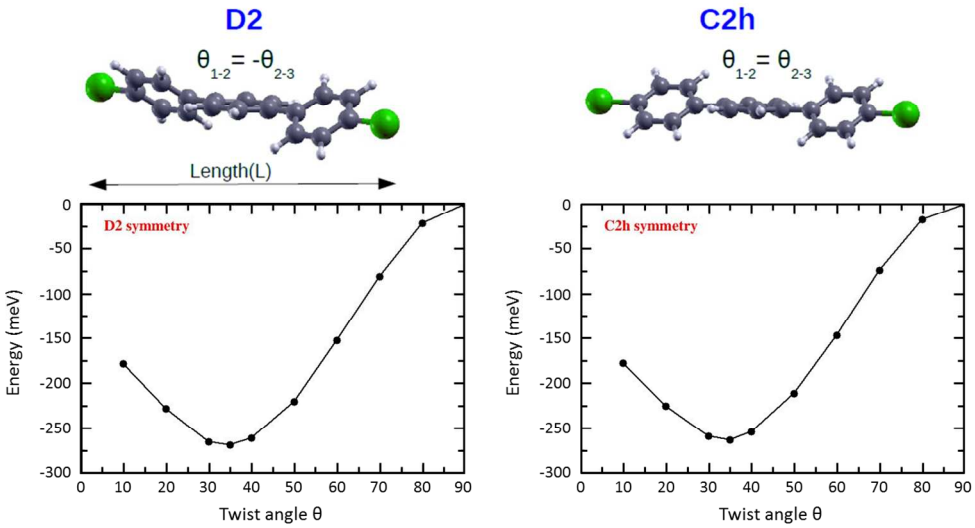

Figure S3: Energy curves of the optimized molecule as function of the twist angle for the D2 and C2h conformations. Left and right panels correspond respectively to the D2 and C2h symmetry cases.

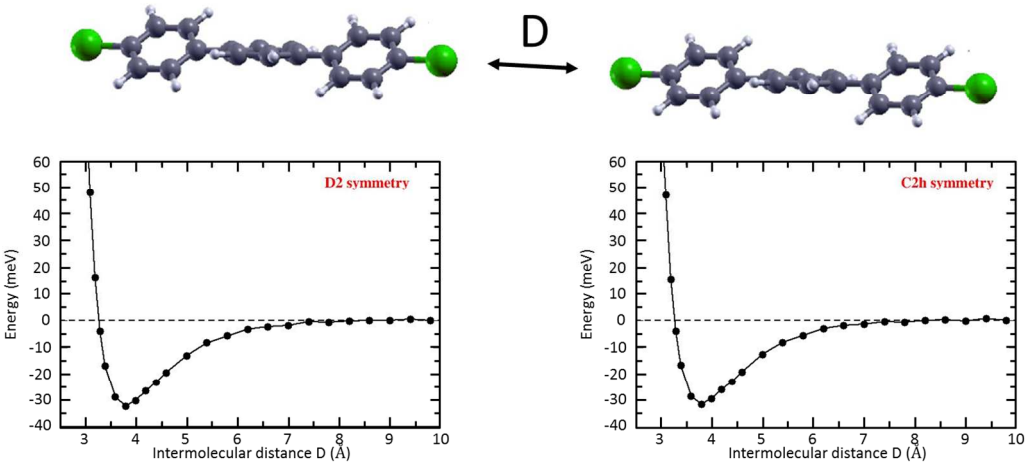

Figure S4: Energy curves obtained for two facing molecules aligned along the same axis as function of the intermolecular Br-Br distance (D). Left and right panels correspond respectively to the D2 and C2h symmetry cases.

Note 2: Supramolecular and polymeric LEED patterns

Supplementary figure 4 and 5 explain how the lack of phase relation between adjacent supramolecular and polymeric chains lead to the apparition of stripes running along the [-1,1,0] direction in LEED. In both cases, the reciprocal lattices corresponding to the different possible phases between neighboring chains are calculated. The sum of these different lattices give rise to a striped pattern, as the ones observed experimentally.

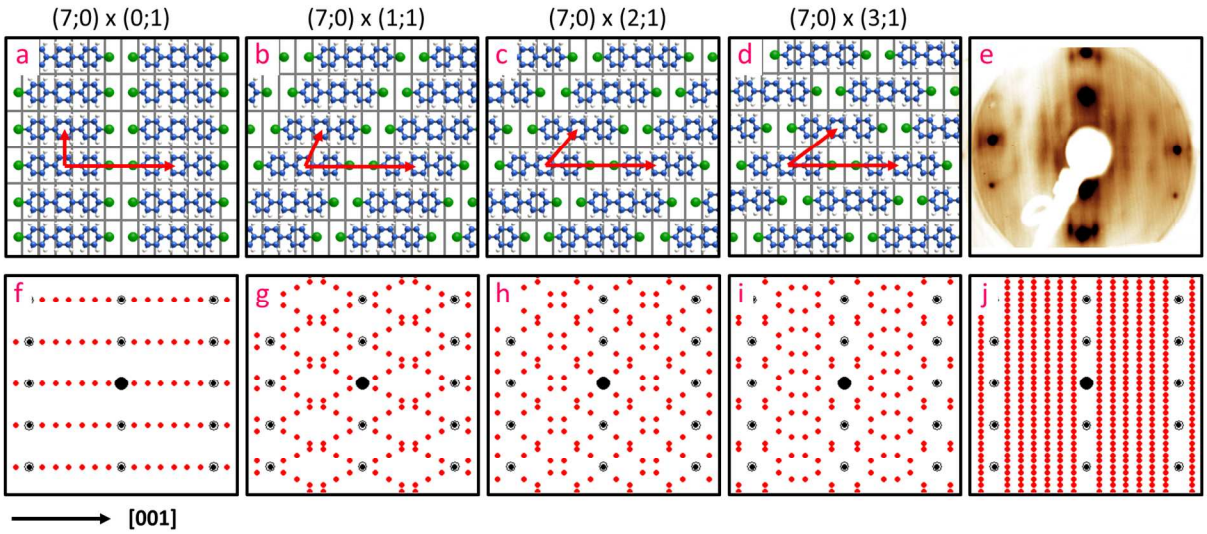

Figure S5: Supramolecular LEED pattern. (a-d) Schematic representations of four unit cells arising from different spatial shifts between neighbouring supramolecular DBTP chains. (f-i) Reciprocal lattices respectively corresponding to (a-d). The back spots correspond to the signature of the TiO_2 surface. (e) LEED pattern (45eV) measured for the supramolecular phase; (j) Superposition of the other four reciprocal lattices (f-i).

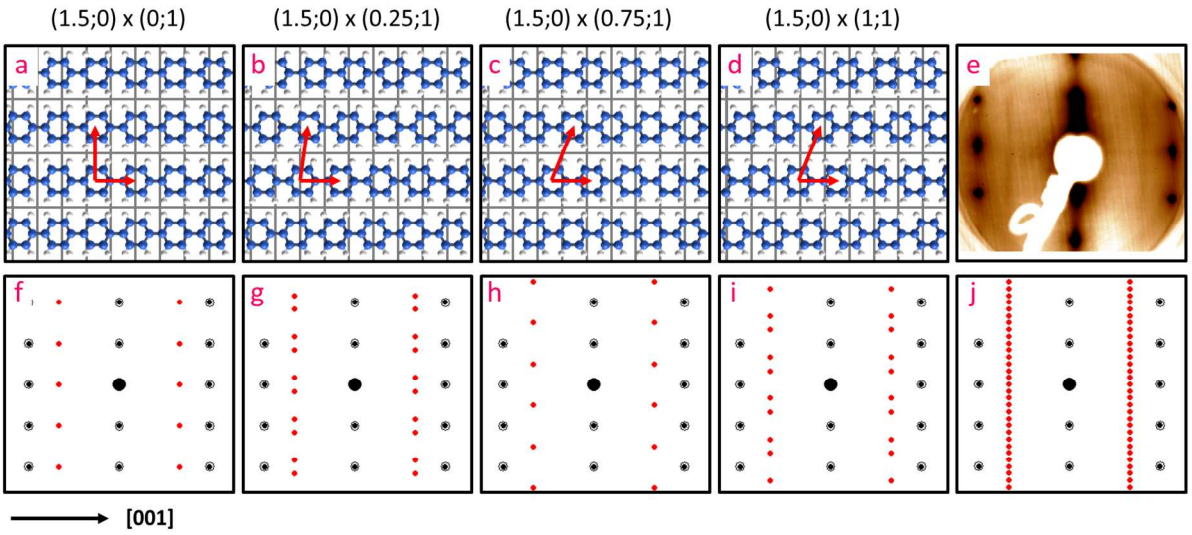

Figure S6: Polymeric LEED pattern. (a-d) Schematic representations of four unit cells arising from different spatial shifts between neighbouring PPP chains. (f-i) Reciprocal lattices respectively corresponding to (a-d). The black spots correspond to the signature of the TiO_2 surface. (e) LEED pattern (44eV) measured for the polymeric phase; (j) Superposition of the other four reciprocal lattices (f-i).

Note 3: Phase transition in LEED

Supplementary Figure 6 presents the LEED patterns measured on a sample saturated with DBTP at room temperature and post-annealed to different temperatures. The signature of the supramolecular phase remains unchanged until 450K. At 490K, the supramolecular features vanish and only the spots of the clean surface are visible.

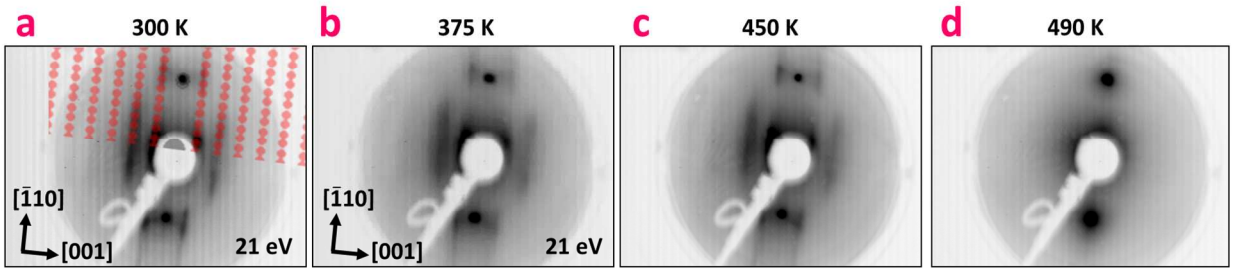

Figure S7: Temperature phase transition of DBTP followed by LEED. LEED patterns (21 eV) acquired for 1ML of DBTP evaporated on a sample held at RT (a) and post-annealed at 375 K (b), 450 K (c) and 490 K (d). The supramolecular reciprocal network deduced from figure S5 is overprinted on the left panel.

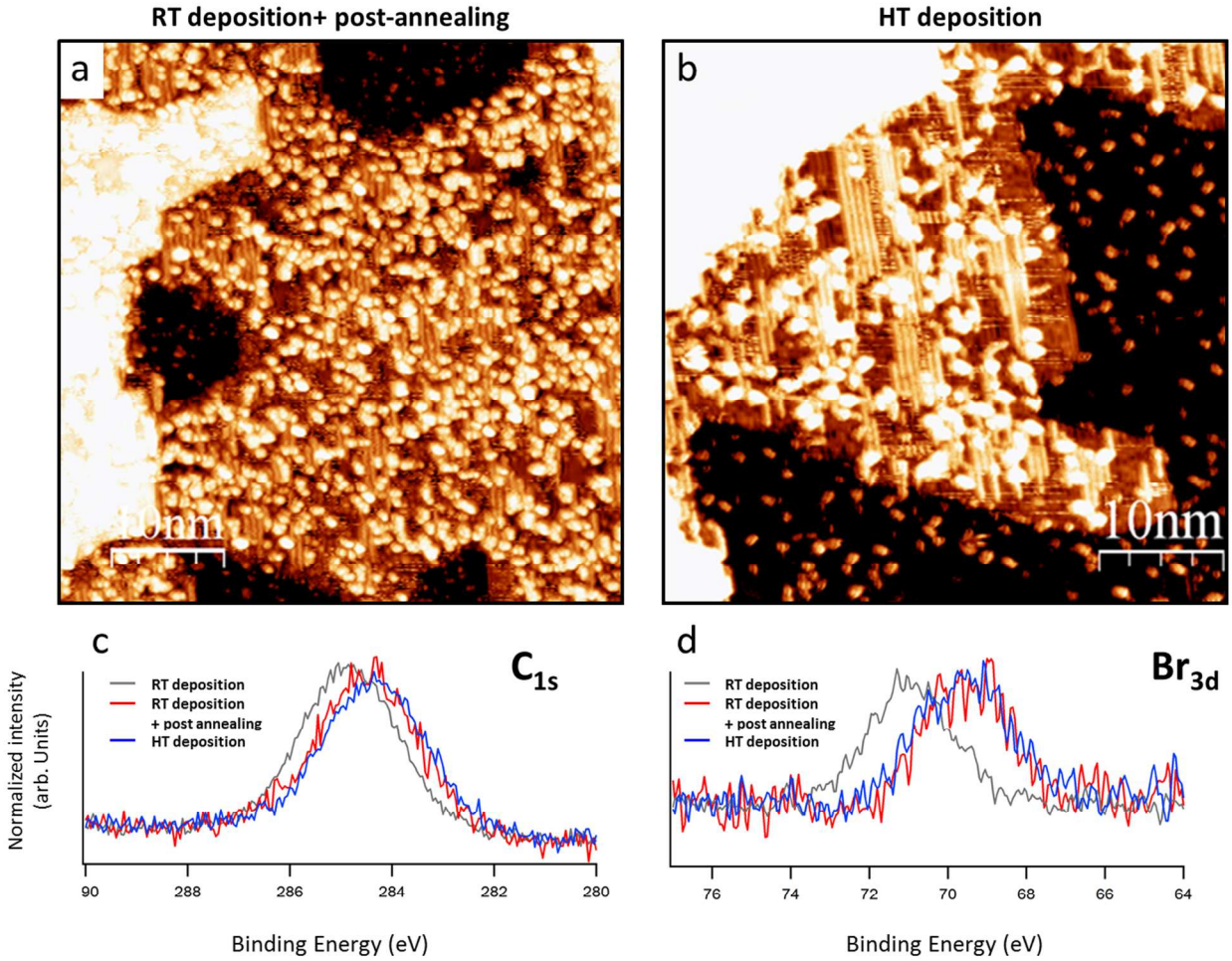

Figure S8: Comparison between post-annealed room temperature preparation and high temperature deposition. (a,b) STM images of the surface after (a) deposition of molecules at room temperature followed by post annealing over 520K, and (b) after deposition of molecules with the substrate kept at high temperature; (c,d) XPS measurements of C1s and Br3d core levels as function of preparation.

Supplementary references.

1. Kresse, G.; Furthmüller, J. *Comput. Mater. Sci.* **1996**, *6*, 15−50.
2. Kresse, G.; Furthmüller, J. *Phys. Rev. B* **1996**, *54*, 11169−11186.
3. Kresse, G.; Hafner, J. *Phys. Rev. B* **1993**, *47*, 558−561.
4. Blöchl, P. E. *Phys. Rev. B* **1994**, *50*, 17953−17979.
5. Klimeš, J. ; Bowler, D. R.; Michaelides, A. *Phys. Rev. B* **2011**, *83*, 195131 .